JCB Article

Regulation of KinI kinesin ATPase activity by binding to the microtubule lattice

Carolyn A. Moores,[1] Mohammad Hekmat-Nejad,[2] Roman Sakowicz,[2] and Ronald A. Milligan[1]

[1]Department of Cell Biology, The Scripps Research Institute, La Jolla, CA 92037
[2]Cytokinetics Inc., South San Francisco, CA 94080

KinI kinesins are important in regulating the complex dynamics of the microtubule cytoskeleton. They are unusual in that they depolymerize, rather than move along microtubules. To determine the attributes of KinIs that distinguish them from translocating kinesins, we examined the ATPase activity, microtubule affinity, and three-dimensional microtubule-bound structure of a minimal KinI motor domain. Together, the kinetic, affinity, and structural data lead to the conclusion that on binding to the microtubule lattice, KinIs release ADP and enter a stable, low-affinity, regulated state, from which they do not readily progress through the ATPase cycle. This state may favor detachment, or diffusion of the KinI to its site of action, the microtubule ends. Unlike conventional translocating kinesins, which are microtubule lattice–stimulated ATPases, it seems that with KinIs, nucleotide-mediated modulation of tubulin affinity is only possible when it is coupled to protofilament deformation. This provides an elegant mechanistic basis for their unique depolymerizing activity.

Introduction

Microtubules are central components of the cytoskeleton and play key roles in a great many cellular functions (Nogales, 2000). Microtubules polymerize and depolymerize dynamically, controlled by the guanine nucleotide bound to the αβ-tubulin heterodimers from which the microtubule wall is built; GTP bound to the dimer favors microtubule growth, whereas its hydrolysis to GDP results in microtubule shrinkage (Desai and Mitchison, 1997). This switching between phases of growth and shrinkage is called dynamic instability and occurs stochastically in solutions of pure tubulin. In the cell, the polymeric state of tubulin, critical for cell division, cell movement, and intracellular transport, cannot be allowed to fluctuate at random, so many cellular factors are employed to control this dynamic behavior (Walczak, 2000).

Kinesin superfamily members bind to microtubules and use their ATPase cycle to drive motor activity (Vale and Fletterick, 1997). The cellular functions of these motor proteins are extremely diverse but the presence of a motor core (containing both ATPase and microtubule-binding activities) defines them as kinesins (Goldstein and Philp, 1999). It has been shown for a number of kinesins that their diverse functions are conferred by sequences outside their motor cores. This is not surprising, as these motor cores comprise the most highly conserved regions in all kinesins (Kim and Endow, 2000). What is surprising, however, is that the activity of one of the most functionally divergent of kinesins, the microtubule-depolymerizing KinIs, resides within their conserved motor cores (Moores et al., 2002).

KinIs, including MCAK (Maney et al., 1998) and XKCM1 (Kline-Smith and Walczak, 2002), are involved in the control of microtubule dynamics in cells. These proteins are essential for the accurate segregation of chromosomes during cell division (Hunter and Wordeman, 2000), and their localization to the ends of microtubules, especially at the kinetochore and spindle poles (Walczak et al., 1996; Maney et al., 2000), places them in exactly the right place for this role. Cellular and in vitro studies have shown that KinI motors depolymerize microtubules (Desai et al., 1999; Homma et al., 2003; Hunter et al., 2003), releasing tubulin dimers from microtubule ends.

KinIs are so-named because their kinesin motor core is located internally within their primary sequences (Vale and Fletterick, 1997). This is in comparison to KinN and KinC motors, which have their motor cores in NH_2- and COOH-terminal positions, respectively. In vertebrate KinIs, a cellular localization domain and the class-specific neck sequences are found NH_2 terminal to the motor core, and the putative dimerization domain is located COOH terminally (Maney

The online version of this article includes supplemental material.

Address correspondence to Ronald A. Milligan, Department of Cell Biology, CB227, The Scripps Research Institute, 10550 N. Torrey Pines Road, La Jolla, CA 92037. Tel.: (858) 784-9827. Fax: (858) 784-2749. email: milligan@scripps.edu

Key words: kinesin; microtubules; cryoelectron microscopy; protein structure; mitosis

et al., 1998). It was originally hypothesized that the motor core's central location was the key to determining the unique depolymerizing function of KinIs. This was subsequently shown not to be the case, and, in fact, the KinI motor core itself is capable of microtubule depolymerization (Moores et al., 2002; Ovechkina et al., 2002). The KinI motor performs this depolymerization by inducing a conformational change in its microtubule substrate when it binds ATP (Desai et al., 1999; Moores et al., 2002). KinI-induced tubulin release is brought about as the motor bends the αβ-tubulin dimer away from the constraints of the microtubule lattice. ATP binding has also been shown to be the critical point in the stepping activity of KinN kinesins (Rice et al., 1999) and in minus end–directed movement of KinCs (Wendt et al., 2002), suggesting that all kinesins use the energy of ATP binding to do work. However, given the unusual properties of KinIs, it was uncertain whether their motors would interact with microtubules using a different mechanism than motile kinesins or whether, indeed, all kinesins share a conserved mode of microtubule interaction.

We wanted to know to what extent the well-characterized microtubule binding properties of other kinesin family members are shared by the KinI motors. We therefore used biochemical and structural methods to characterize the motor core of a KinI from *Plasmodium falciparum* (pKinI) and identified steps in the motor's ATPase cycle that are critically involved in both its depolymerizing function and its regulation.

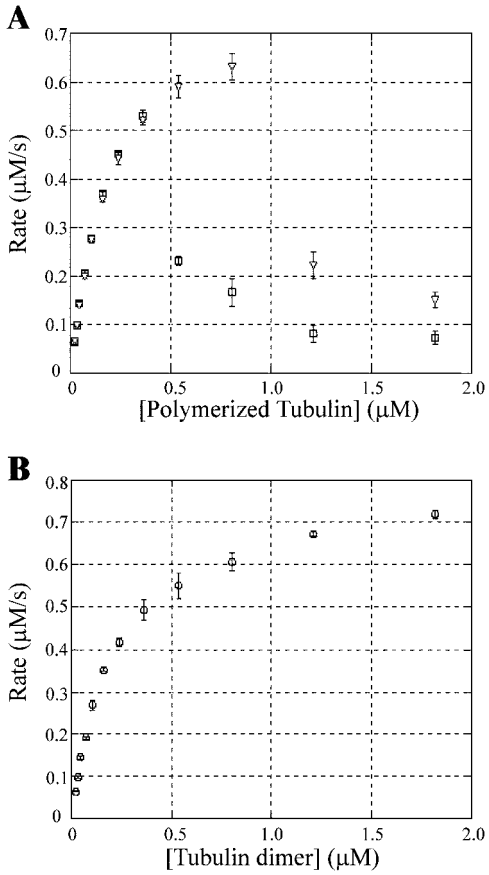

Figure 1. **Steady-state ATPase activity of pKinI.** (A) Initial rate of ATP hydrolysis as a function of varying concentrations of unsheared (□) and sheared (▽) taxol-stabilized microtubules with 0.25 μM pKinI; $n = 3$. (B) Initial ATPase rate with varying concentrations of GDP-tubulin dimers with 0.25 μM pKinI; $n = 2$.

Results

Microtubule-stimulated ATPase activity of pKinI

We previously showed that a protein construct consisting of only the motor core (i.e., lacking NH_2-terminal neck residues and residues COOH terminal to the structurally defined motor core; Sack et al., 1999) of a KinI from *Plasmodium falciparum* (pKinI) was capable of depolymerizing microtubules (Moores et al., 2002). To further characterize the unique behavior of KinI kinesins, we first examined the steady-state microtubule-stimulated ATPase activity of this construct (Fig. 1 A). In the presence of taxol-stabilized microtubules, pKinI ATPase activity reached a maximum rate of 0.53 μM/s. However, we also saw inhibition of ATPase activity at high microtubule concentrations, a behavior not observed for other kinesin family members (Fig. S1, available at http://www.jcb.org/cgi/content/full/jcb.200304034/DC1; Huang and Hackney, 1994; Rogers et al., 2001). It has been shown that although KinI-catalyzed depolymerization occurs only from the ends of microtubules, KinIs also bind along the microtubule lattice (Wordeman et al., 1999; West et al., 2001; Moores et al., 2002; Hunter et al., 2003). As the number of lattice binding sites increases more rapidly than the number of microtubule ends with increasing microtubule concentration, we wondered whether lattice binding caused the inhibition of the motor ATPase. To test this idea, we sheared taxol-stabilized microtubules to produce twice as many ends as in a nonsheared population and used this preparation in the ATPase assay. The sheared microtubules stimulated pKinI ATP hydrolysis to about the same extent as the unsheared microtubules (maximum rate of 0.63 μM/s), but the onset of inhibition was displaced to higher microtubule concentrations (Fig. 1 A). Furthermore, sheared microtubules that were allowed to reanneal at room temperature exhibited inhibitory activity similar to the unsheared microtubules (unpublished data). These results strongly suggest that the ATPase activity of the pKinI motor core is stimulated by microtubule ends and is substantially reduced by motor binding to lattice sites in the body of the microtubule.

We next asked whether the pKinI ATPase activity was also stimulated by unpolymerized GDP-tubulin heterodimers (Fig. 1 B). There were two striking results from this experiment. First, the maximum rate of hydrolysis was comparable to that found with sheared microtubules (0.78 μM/s for tubulin heterodimers, 0.63 μM/s for sheared microtubules), and second, the inhibition seen at high concentrations of polymerized tubulin was absent. These data show that unpolymerized tubulin heterodimers are as effective as microtubule ends in stimulating the pKinI ATPase, and also seem to lend support to the idea that hydrolysis occurs on the heterodimer after it has detached from the microtubule end (Desai et al., 1999). In addition, as the only difference between the tubulin substrates in Fig. 1 (A and B) is that the tubulin is polymerized in Fig. 1 A, we conclude that pKinI ATPase activity is inhibited by binding to the microtubule lattice. Such inhibition has not been observed with other ki-

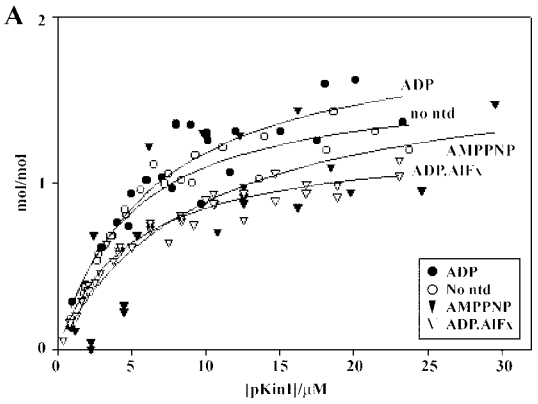

B

KINESIN CONSTRUCT	Kd of each nucleotide state/μM			
	ADP	no ntd	AMPPNP	ADP.AlFx
pKinI motor core	6.4 (± 1.4)	4.8 (± 0.7)	9.4 (± 5.5)	4.9 (± 0.5)
rat conventional kinesin motor core + neck (rkin340 +GFP) (Rogers et al., 2001)	6.7	0.15	0.19	not given

Figure 2. **Characterization of the microtubule binding affinity of pKinI throughout its ATPase cycle.** (A) A rectangular hyperbola was fit to data acquired from cosedimentation assays of taxol-stabilized microtubules with pKinI complexed with each of ADP, no nucleotide, AMPPNP, and ADP.AlFx. (B) Comparison of the Kd values for each of the nucleotide states of pKinI with those of a conventional kinesin construct (Rogers et al., 2001). The numbers in brackets are the standard error of the fit of the binding curve.

nesin motors, whose ATPase is stimulated by lattice binding in the course of their motility cycle.

Microtubule binding properties of pKinI

In conventional kinesin, the progression through the ATPase cycle is accompanied by changes in the affinity of the motor for the microtubule lattice. These changes in affinity enable processive movement; each of the two heads cycles coordinately between weakly and strongly bound states to allow sequential stepping along the microtubule lattice (Ma and Taylor, 1997). If lattice binding inhibits the pKinI ATPase, as suggested by the results described in the previous section, then we would not expect to see nucleotide-dependent affinity changes with this motor. To test this idea, we trapped the pKinI motor at various stages of its ATPase cycle with ADP, no nucleotide, AMPPNP (mimicking the ATP-bound state), and ADP.AlFx (mimicking an ADP.Pi-like transition state) and incubated a range of concentrations of each of these motor–nucleotide complexes with a constant concentration of taxol-stabilized microtubules. After incubation, we separated free motor from motor–microtubule complexes by centrifugation. We used this sedimentation assay to determine the affinity of the motor in each nucleotide state for the microtubule lattice (see Materials and methods).

In common with all characterized kinesins, the binding of pKinI to the microtubule lattice saturates at a stoichiometry of one motor for every αβ-tubulin heterodimer (Fig. 2 A). However, the binding affinity of pKinI for the microtubule lattice was essentially the same for each of the nucleotide states examined, in dramatic contrast to conventional kinesin whose affinity for the microtubule increases by a factor of ~45 on ADP release (Fig. 2 B; Crevel et al., 1996; Rogers et al., 2001). As this change in affinity is not observed with pKinI, the simple interpretation of our binding data is that all four "nucleotide states" examined are locked in the same low-affinity structural state. Our results suggest that this structural state is ADP-like, as there is little change in affinity between the ADP and the putative nucleotide-free state (the first transition in the motor–microtubule cycle of interaction).

Structure of pKinI bound to the microtubule lattice

To see if the pKinI–lattice interaction geometry might provide an explanation for the unique binding properties we had observed, we next used cryo-electron microscopy and helical image analysis to calculate 20–30-Å resolution three-dimensional maps of taxol-stabilized microtubules decorated with pKinI in putative ADP, nucleotide free, AMPPNP,

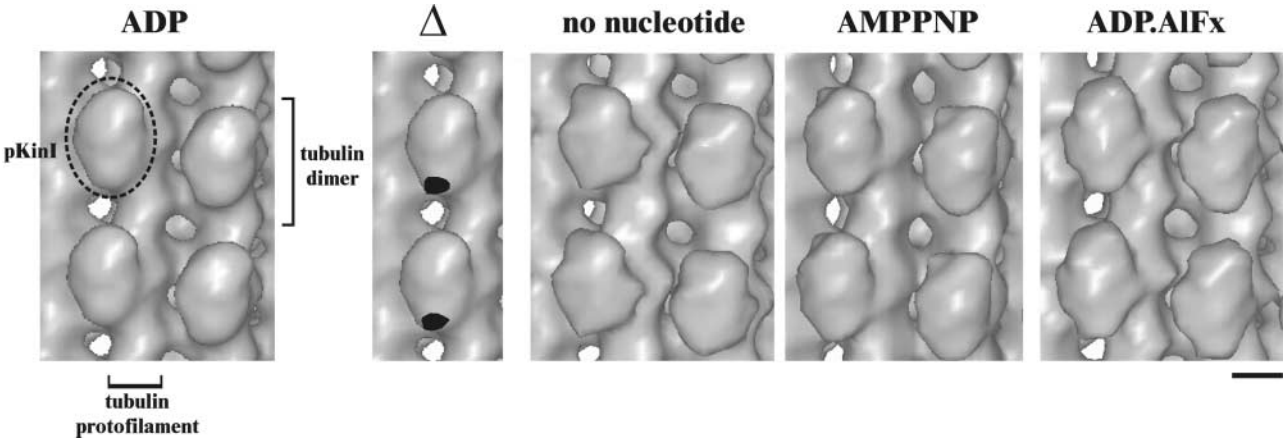

Figure 3. **Three-dimensional maps of the pKinI–microtubule complexes.** Side views of each pKinI–nucleotide microtubule complex with four motor heads displayed and the microtubule plus end at the top of the figure. Each map is contoured to give the same volume for the microtubule portion of the map; thus, slight differences in the degree of decoration in each sample likely contribute to the superficial differences in the motor seen in most of the nucleotide states. The position of the statistically significant ADP release–induced conformational change (Δ) is shown in black superimposed on the pKinI-ADP microtubule map, and is located at the minus end of the motor density close to the microtubule surface. Bar, 30 Å.

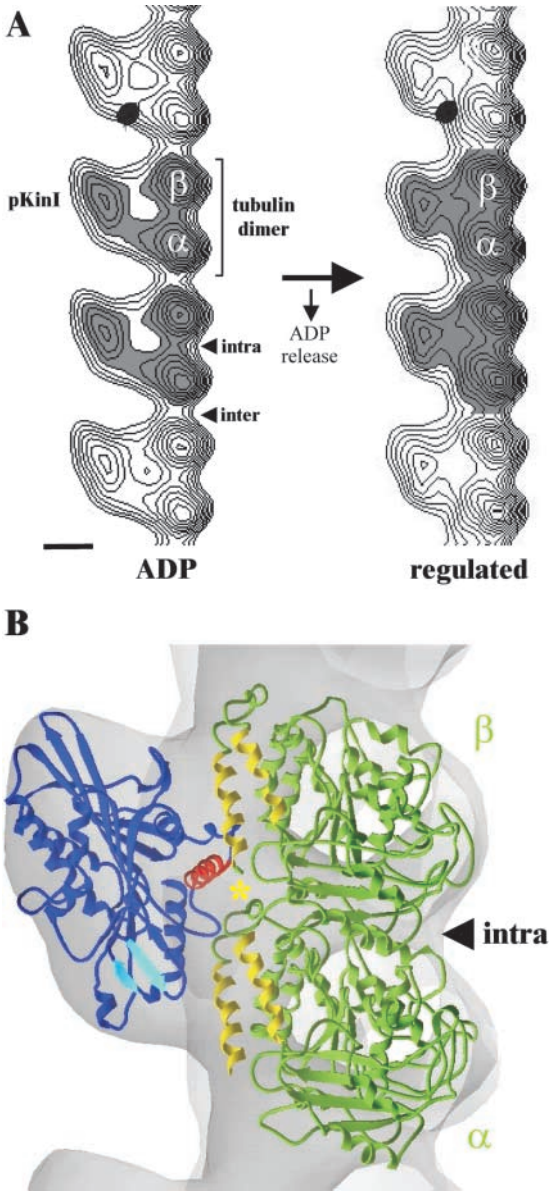

Figure 4. **The ADP release–dependent conformational change in pKinI is close to KinI class-specific sequence insertions.** (A) Two-dimensional projections of single protofilaments from pKinI-ADP and pKinI-nucleotide-free microtubule maps showing the position of the ADP release–dependent conformational change. In each nucleotide state, the projection at higher contour is shaded. The position of the peak of significant difference between the two maps is shown in black and identifies additional positive density in the presence of ADP, and is absent when it is released. The microtubule plus end is at the top of the figure. Bar, 30 Å. (B) Pseudo-atomic model of the pKinI–microtubule complex. The structure of GTP-tubulin (in green; Löwe et al., 2001) fits well within the microtubule portion of the pKinI-ADP microtubule map (gray). The motor makes its main contact with the microtubule surface by interacting with the COOH-terminal helices H11 and H12 of α- and β-tubulin (in yellow). The position of the disordered β-tubulin COOH terminus, essential for pKinI depolymerization, is marked with an asterisk. The structure of human conventional kinesin (Kull et al., 1996) fits reasonably well within the pKinI motor density (in blue), and revealed the positioning of the kinesin relay helix (in red) over the intradimer interface (arrowhead). Shown in cyan is the loop 2 β-sheet structure into which KinI-specific residues are inserted; with this insertion, the β-sheet structure likely lies close to the microtubule surface, suggesting a critical role for these residues in depolymerization.

and ADP.AlFx states (see Materials and methods). Layer line data for these maps are included as online supplemental material (Fig. S2, available at http://www.jcb.org/cgi/content/full/jcb.200304034/DC1). In the three-dimensional maps (Fig. 3), the general features of the pKinI–microtubule complex are very similar to those of other members of the kinesin superfamily (e.g., Sosa et al., 1997; Rice et al., 1999; Kikkawa et al., 2001). In fact, there were no significant differences between maps of pKinI-decorated microtubules and maps of conventional kinesin motor domain–decorated microtubules. The density corresponding to the pKinI motor sits at high microtubule radius on the crest of each protofilament. Consistent with the 1:1 motor/tubulin dimer stoichiometry determined by the cosedimentation assay, the motors are spaced every 80 Å along each protofilament, corresponding to a binding site on each αβ-tubulin heterodimer. Thus, sequence homology in the motor domains of KinN, KinC, and KinI motors dictates a common geometry of microtubule lattice interaction, despite the very different functional attributes of these kinesin classes.

A conformational change on ADP release

Visual comparisons of the three-dimensional maps reveal only subtle variations in the surface features of the pKinI density between each of the nucleotide states (Fig. 3). To detect nucleotide-mediated structural rearrangements within the motor, we used *t* tests to reveal statistically significant differences between the maps (Milligan and Flicker, 1987). Consistent with the absence of affinity changes, no statistically significant differences in structure were observed when we compared the putative nucleotide-free, AMPPNP, and ADP.AlFx three-dimensional maps (unpublished data). However, we did detect a statistically significant difference ($P < 0.0005$) between the ADP and nucleotide-free motor–microtubule complexes (Figs. 3 and 4). The difference is additional positive density in the ADP map. It does not coincide with the nucleotide binding pocket and so is most likely due to a conformational change in the motor rather than being due to ADP itself (which we do not expect to detect at ~20-Å resolution anyway). Projections of single protofilaments (with attached motors) cut from the three-dimensional maps reveal the complex in profile and show that the statistically significant difference peak lies at the minus end of the motor–microtubule interface (indicated in black in Fig. 4 A). A change in connectivity between the motor and the underlying protofilament is also evident in this view (compare shaded densities in Fig. 4 A) and may be due to reorganization of the interface in the transition between these states.

Ordinarily, we would interpret differences in these two structures to be indicative of conformational changes resulting from the ADP release step in the enzymatic cycle, because we observe microtubule-stimulated ADP release by pKinI under our experimental conditions (Fig. S3, available at http://www.jcb.org/cgi/content/full/jcb.200304034/DC1). However, in the case of pKinI, examined here, the structural change (which is unequivocally revealed by statistical difference mapping) is not accompanied by the expected increase in binding affinity (Fig. 2). These apparently conflicting data suggest that the putative nucleotide-free state we have visualized is a previously unobserved state. It is clearly different

from the ADP state, but it is not the expected high-affinity, nucleotide-free state seen for other kinesins; it appears to be intermediate between the ADP and nucleotide-free states. Furthermore, the lack of any subsequent structural changes (at the resolution of this study) or affinity changes suggests that this pKinI–microtubule intermediate is stable, even in the presence of nucleotide analogues that, under other circumstances (e.g., Moores et al., 2002), elicit the depolymerizing activity of the motor. Together the data argue in favor of a model in which pKinI bound to the microtubule lattice is arrested in a low-affinity binding state and unable to proceed through the ATPase cycle.

A pseudo-atomic model for the complex

A modeling approach allowed us to identify the important points of contact between the proteins and to identify structural elements that might be involved in defining and regulating motor-mediated depolymerization. We docked the tubulin heterodimer structure (Löwe et al., 2001) into the microtubule portion of the three-dimensional map and used the structure of conventional kinesin (Kull et al., 1996) to represent the homologous pKinI motor domain (Fig. 4 B). As has been observed in a number of similar docking experiments, the motor bridges the two tubulins of the heterodimer with its mechanistically important relay helix (α6, red in Fig. 4 B) lying close to the intradimer interface (Vale and Milligan, 2000; Kikkawa et al., 2001). The likely location of the COOH terminus of β-tubulin (Fig. 4 B, yellow asterisk), underneath the motor density and in close proximity to the relay helix, is particularly significant, because its presence is essential for KinI-mediated depolymerization (Moores et al., 2002; Niederstrasser et al., 2002).

From sequence comparisons, the biggest cluster of KinI class-specific residues (13 residues in pKinI) is inserted in the loop 2 β-sheet structure close to the microtubule surface at the minus end of the motor (Fig. 4 B, cyan). Although we do not know the conformation of this insert, it is ideally placed to participate in the binding interface. The docking places this class-specific insert, which is presumably extremely important in specifying the depolymerization activity of the motor, very close to the position of the statistically significant difference peak described earlier. Thus, the case for the structural difference during the ADP release step being functionally relevant is supported by observations from modeling experiments.

Discussion

Sequence conservation in the motor domain throughout the kinesin superfamily is high and has given rise to the idea that the actions of the catalytic core are conserved and that the wide range of cellular functions performed by these motors are largely specified by elements outside the core (Goldstein and Philp, 1999; Vale and Milligan, 2000). KinI kinesins are particularly notable in that they do not conform to this idea. Despite a high level of sequence similarity with other classes, the motor core defines the functionality of the molecule in catalyzing microtubule depolymerization (Moores et al., 2002). To help understand KinI function, it is important to determine which properties these motors share with other kinesins and which relate to their specific depolymerization activity. Full-length KinI molecules have three distinct biochemical properties: (1) ATP-dependent microtubule depolymerization (Desai et al., 1999; Hunter et al., 2003), (2) binding along the microtubule lattice (Wordeman et al., 1999; West et al., 2001; Hunter et al., 2003), and (3) tubulin-stimulated ATPase activity (Hunter et al., 2003). Our minimal motor, pKinI, has all these properties and is therefore an excellent model for dissecting the molecular mechanism of the protein. The minimal pKinI motor we have used presumably represents the smallest functional unit of these molecules, so any differences in the degree to which these KinI-specific properties are present in this minimal motor, compared with a full-length molecule, provide insight into the role of the various elements outside the motor domain.

Previously, we examined pKinI-mediated microtubule depolymerization and showed that bending of protofilaments at microtubule ends was coupled to the ATP binding step and was dependent on the β-tubulin COOH terminus (Moores et al., 2002; Niederstrasser et al., 2002). Here we have focused our attention on investigating lattice binding and stimulation of the ATPase activity. Our goal was to understand what roles these attributes play in the normal function of the KinI depolymerizing machine.

The KinI ATPase and free tubulin

We first investigated the stimulation of the pKinI steady-state ATPase by unpolymerized GDP-tubulin, by microtubule ends, and by the microtubule lattice. Our data (Figs. 1 and 2), as well as those of Hunter et al. (2003), demonstrate that tubulin at microtubule ends or free in solution stimulates the ATPase activity of both the minimal motor and the full-length protein (Hunter et al., 2003), albeit to different extents. Although both sets of results tell us that ATP binding, hydrolysis, and product release by KinI can take place on the free heterodimer, unpolymerized tubulin is very unlikely to be an in vivo substrate for KinI kinesins. Rather, its ability to stimulate KinI motor ATPase activity probably reflects its structural similarity to the bent tubulin conformation, which the motor itself induces as part of the depolymerization mechanism. The likely structural and dynamic similarities between depolymerizing and depolymerized tubulin necessitates evolution of a mechanism to focus KinI activity at the former and not the latter. The differing behaviors of full-length and minimal motors may hint at such a mechanism. Stimulation of full-length KinI ATPase by GDP- or GTP-tubulin heterodimers is ∼35-fold lower compared with that with polymer (Hunter et al., 2003), whereas stimulation of the pKinI minimal motor ATPase by GDP-tubulin is comparable to that observed with polymer. This difference in the degree of ATPase stimulation suggests that structural elements outside the motor domain act to favor the microtubule end–stimulated ATPase of the full-length molecule.

Lattice inhibition of the KinI ATPase

A second result from these data is that the pKinI ATPase is inhibited by binding to tubulin that is held rigidly in the microtubule lattice relative to the stimulation observed at microtubule ends (or by free tubulin). Consistent with down-

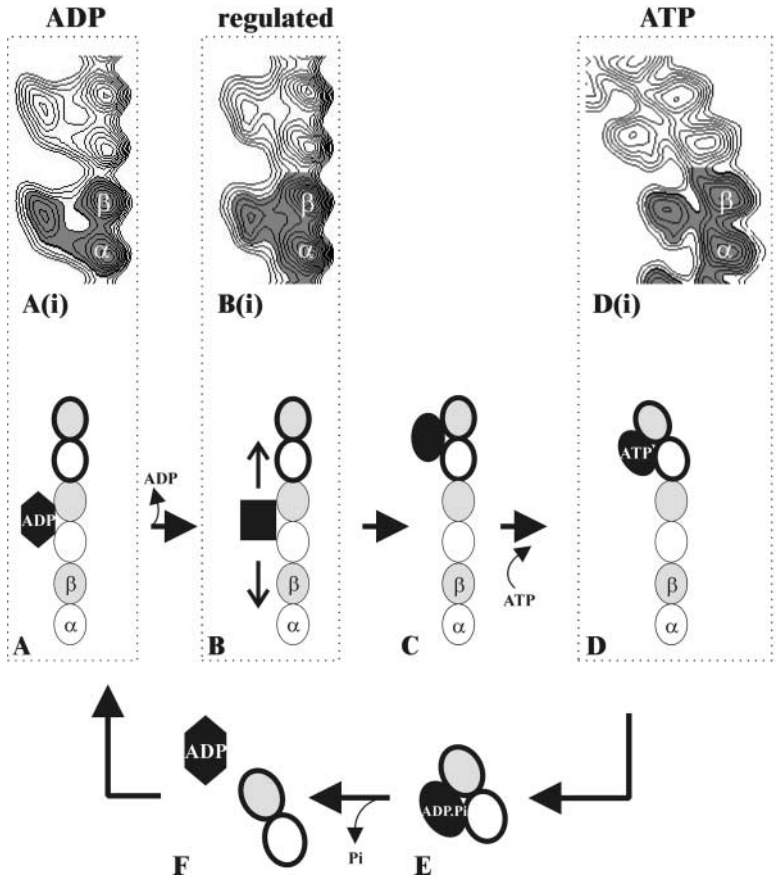

Figure 5. **Model for regulation and microtubule depolymerization of KinIs.** A single microtubule protofilament (shaded/unshaded) with attached KinI motor (black) is shown diagrammatically in the central panels. The bold ellipses identify the terminal tubulin heterodimers that are structurally distinct from lattice tubulins. (A) KinI.ADP forms an initial collision complex (black polygon) with the microtubule lattice. An equivalent view of the EM map is shown in A(i). The KinI.ADP microtubule affinity is comparable to that of conventional kinesin. (B) ADP is released (Fig. S3, available at http://www.jcb.org/cgi/content/full/jcb.200304034/DC1), but the KinI microtubule affinity is unchanged, and the ATPase is inhibited. This low-affinity regulated state (black square) may allow equilibrium to new lattice positions by motor dissociation–reassociation, or by one-dimensional diffusion of the motor along the protofilament (Hunter et al., 2003), until the motor reaches a terminal tubulin heterodimer. An equivalent view of the regulated KinI–lattice complex is shown in B(i). The statistically significant differences between A(i) and B(i) (Figs. 3 and 4) are attributable to a structural change mediated by ADP release (black polygon to black square). (C) The conformation of the terminal dimer permits establishment of a high-affinity, nucleotide-free state (black ellipse). This conformation has not been observed by EM. (D) ATP binding to the high-affinity complex is coupled to outward curling of the terminal tubulin dimer. The structure of the curled or ring-like oligomeric complex, D(i), has been described previously (Moores et al., 2002). Tubulin–pKinI.AMPPNP rings are 13-fold symmetric. Comparing maps in which 13-fold symmetry (averaging pKinI–heterodimers) or 26-fold symmetry (effectively averaging α and β tubulins) demonstrates that bending occurs both at the intradimer contacts (where pKinI is located) and at the interdimer contacts along the protofilament (unpublished data). This implies that there are allosteric changes in the tubulin as a result of bending by KinIs. As curled oligomers are stable in the presence of a nonhydrolyzable ATP analogue and not seen with an ADP.Pi-like analogue, we argue that ATP hydrolysis must occur on the curled protofilament and be coupled to breakage of the interdimer contacts to release a KinI–heterodimer complex (E). It is envisioned that the final step in the cycle, Pi release, is coupled to subunit dissociation (F).

regulation of the motor ATPase when bound to the lattice, higher total polymer concentrations are required to observe the inhibitory effects if the number of microtubule ends (productive binding sites) is increased by shearing the microtubules (Fig. 1 A). Data obtained by Hunter et al. (2003) also demonstrated very low lattice-stimulated ATPase activity of full-length protein. Although our data and those of Hunter et al. (2003) differ in terms of the magnitude of the effect, it is clear that lattice binding does not elicit the same dramatic enzymatic stimulation as microtubule ends. Such inhibition or down-regulation is extremely uncharacteristic of kinesins (Fig. S1; Huang and Hackney, 1994; Rogers et al., 2001), which are generally molecules whose ATPase activity is stimulated by polymerized tubulin and coupled to linear motion along the microtubule lattice.

Determination of the affinity of pKinI–nucleotide complexes for the microtubule lattice shed further light on the lattice binding phenomenon (Fig. 2). In keeping with the idea that lattice binding inhibits the ATPase, we saw essentially no difference in the microtubule affinity of four pKinI–nucleotide complexes. Again, this is unlike the translocating kinesins whose affinities for the microtubule lattice are greatly modulated by, and coupled to, their nucleotide state. Together, the ATPase and affinity data suggest that the KinI ATPase is severely inhibited by binding to the microtubule lattice.

Visualization of the regulated state

Our cryo-EM investigation of the microtubule-bound pKinI–nucleotide complexes showed that the initial collision complex (MT–pKinI.ADP) and a subsequent nucleotide-free state are structurally distinct. This transition is not accompanied by the dramatic increase in motor–microtubule affinity seen in the translocating kinesins; therefore, we postulate that ADP release from a lattice-bound KinI induces formation of a regulated state. As there are no further structural or affinity changes observed with ATP or ADP.Pi analogues, the regulated state is stable in lattice-bound KinI motors, and progression through the ATPase cycle is inhibited.

A model for KinI action

We have incorporated these data and conclusions into a model describing the interaction cycle of KinIs with microtubules. The cycle begins unremarkably in typical kinesin fashion (Fig. 5 A). The affinity of KinI.ADP for microtubules is weak and comparable to that of other kinesins (Fig. 2 B; Crevel et al., 1996; Rogers et al., 2001). Likewise, the appearance and interaction geometry of pKinI and conven-

tional kinesin interaction with the microtubule lattice are similar (Fig. 5 A(i); Sosa et al., 1997; Rice et al., 1999; Kikkawa et al., 2001).

The next stage in the cycle is ADP release from the complex accompanied by a structural change in the motor (Fig. 5 B). Based on the location of the structural difference (Fig. 3 and Fig. 4 A), and the results of modeling experiments (Fig. 4 B), we argue that it involves a KinI-specific sequence insert in loop 2 at the motor–microtubule interface. However, although lattice interaction accelerates ADP release (Fig. S3), this step is not accompanied by an increase in affinity, nor can ATP-like or ADP.Pi-like analogues subsequently bind. Indeed the ATPase is inhibited (Fig. 1). This behavior distinguishes depolymerizing kinesins from the translocating kinesins where these properties are defining features. We believe that this weakly bound, nucleotide-free state is a regulated state unique to the KinIs, and has evolved for two reasons. First, nonproductive ATP consumption is minimized. Second, maintenance of a weak binding state allows the molecule to "search" for a productive binding site by detachment–reattachment cycles, or by one-dimensional diffusion along the protofilament (Hunter et al., 2003). Irrespective of exactly how it gets there, the KinI ends up at a terminal tubulin heterodimer, where the inhibition is released and presumably a high-affinity, nucleotide-free state can be attained (Fig. 5 C).

What is different about the terminal heterodimer that permits release of the inhibition remains to be determined. However, the data showing pKinI and full-length KinI ATPase stimulation by free heterodimers (Fig. 1 and Hunter et al., 2003, respectively) suggest that structural attributes common to depolymerized tubulin and terminal tubulins of protofilaments may be involved. Terminal tubulins are likely more flexible or conformationally dynamic than those constrained on all sides by the lattice, a situation that perhaps allows induction of structural changes that result in KinI high-affinity binding (Fig. 5 C).

After establishment of the high-affinity, nucleotide-free state at the protofilament end, ATP binding to the complex induces protofilament bending (Fig. 5, D and D(i)). Mimicking this step with a nonhydrolyzable ATP analogue produces stable curved oligomers and ring complexes (Desai et al., 1999; Moores et al., 2002). The curvature is a result, not only of deformation of the intradimer contacts that the KinI interacts with directly, but also of the interdimer contacts by an allosteric mechanism (see legend to Fig. 5). As these curved oligomers are the end result of ATP binding, and are not seen when an ADP.Pi analogue is bound, we conclude that the hydrolysis step takes place in the oligomers and is coupled to their break-up or disassembly (Fig. 5 E). Finally, Pi release is envisioned to induce dissociation of KinI from the released tubulin heterodimer (Fig. 5 F).

In conclusion, the KinI-mediated microtubule depolymerization model we have described provides a good example of coupling between structural and biochemical states; the structure of lattice tubulins effectively regulates the KinI ATPase, maintaining the KinI in a low-affinity, nucleotide-free state and inhibiting progression through the enzymatic cycle. The transition to high-affinity binding is coupled to microtubule end localization of the nucleotide-free depolymerization machine and is a result of the unique, but as yet unknown, conformation of the terminal tubulins. ATP binding is tightly coupled to protofilament bending. The high-affinity ATP-bound state, which is a key step in the cycle of translocating kinesins, can only be established in KinIs in concert with protofilament curvature. Thus, the ability of ATP to bind to the nucleotide-free motor is apparently governed by whether a depolymerizing conformation can (microtubule end) or cannot (microtubule wall) be adopted. Such sensitivity provides an ingenious way for the pKinI motor to regulate its use of ATP so that the enzymatic cycle will only occur when depolymerization can actually happen. ATP hydrolysis must be coupled to curved protofilament breakage and release of KinI–heterodimer complexes from the microtubule ends. Pi release is envisioned to be responsible for KinI dissociation from the tubulin heterodimer. Although the data presented here and elsewhere in the literature (e.g., Desai et al., 1999; Maney et al., 2001; Moores et al., 2002; Niederstrasser et al., 2002; Hunter et al., 2003) provide support for some of the key steps, some aspects of the model remain to be tested.

The best characterized role for KinIs in cells is the regulated depolymerization of spindle microtubules during mitosis. The localization of these motors to cellular structures like the kinetochore (Maney et al., 1998; Walczak et al., 2002) places them in a prime position to be involved in accurate chromatid separation through regulation of spindle microtubule length. However, despite the unique attributes of KinI kinesins, these motors have fundamental properties in common with the other members of the kinesin superfamily, with which they work in concert in the mitotic spindle (Wittmann et al., 2001). This is an example of the economy with which nature has achieved a huge range of function through subtle modulation of a single theme.

Materials and methods

Protein methods

The pKinI motor core construct (residues I68-N396 of PFL2165w, www.tigr.org/tdb/e2k1/pfa1) was expressed and purified as previously described (Moores et al., 2002) and was dialyzed into BrB20 (20 mM Pipes, 2 mM $MgCl_2$, 1 mM EGTA, 1 mM DTT, pH 6.8) before use. Microtubules were polymerized using bovine brain tubulin (Cytoskeleton, Inc.). The tubulin, at a final concentration of 5 mg/ml, was incubated with 80 mM Pipes, pH 6.8, 1.5 mM $MgCl_2$, 8% DMSO, and 2.5 mM GTP (in BrB80 buffer, 80 mM Pipes, pH 6.8, 2 mM $MgCl_2$, 1 mM EGTA) for 30 min at 35°C, after which 1 mM paclitaxel (CalBiochem), dissolved in DMSO, was added.

ATPase assay

The ATPase activity of pKinI was measured using the NADH-coupled system of Huang and Hackney (1994). Initial rates of microtubule- or tubulin-activated ATP hydrolysis by pKinI were determined at room temperature in buffer consisting of 25 mM Pipes, pH 6.8, 2 mM $MgCl_2$, 1 mM EGTA, and 1 mM DTT and with 1.5 mM ATP. In the experiments examining tubulin-dependent ATPase activity, unpolymerized tubulin was cold spun to remove tubulin aggregates and preformed polymers, and subsequently stored on ice until use in the assay. The human mitotic kinesin Eg5 (Turner et al., 2001), which does not exhibit tubulin-stimulated ATPase activity, was used as a control to confirm that no tubulin polymers were present. Microtubules were sheared as described by Hunter et al. (2003), and the effect on the number of microtubule ends was estimated by electron microscopy. The KinN motor Eg5 was used as a control to demonstrate non-inhibited microtubule lattice–stimulated ATPase activity typical of other members of the kinesin superfamily (Fig. S1).

Cosedimentation assay

Cosedimentation assays for determination of binding affinities of the pKinI motor in various nucleotide states were performed as previously described

(Moores et al., 2002), with one modification. To measure the affinity of pKinI for the microtubule lattice as accurately as possible, it is essential to separate microtubules and microtubule-associated ligand from everything else. Some of the pKinI-AMPPNP–tubulin rings are found in the pellet fraction, along with microtubules, under our standard assay conditions, with the centrifugation step performed at 400,000 *g* for 15 min. We therefore used a cushion of 20% sucrose/BrB20 during sedimentation of pKinI-AMPPNP incubated with microtubules, at 15,500 *g* for 15 min. Examination of the supernatant and pellet fractions from this experiment by electron microscopy showed that nearly all of the ring complexes remained in the supernatant fraction, and this allowed us to estimate the affinity of the pKinI-AMPPNP for the microtubule lattice. Failure to completely control where the ring complexes fractionated probably contributes to the larger error in estimating the affinity of pKinI-AMPPNP for microtubules, but spinning at slower speeds resulted in small microtubules being found in the supernatant. For all sedimentation experiments, supernatant (free protein) and pellet (microtubules and microtubule-bound protein) fractions were separated after centrifugation and analyzed by SDS-PAGE, and the protein bands in each fraction were visualized by Coomassie blue. The intensity of the gel bands was quantitated using a Molecular Dynamics densitometer equipped with ImageQuant, and the binding curves were calculated using a rectangular hyperbolic fit with Sigmaplot (SPSS Inc.).

Preparation of frozen grids for cryo-electron microscopy

Taxol-stabilized microtubules at 2.5 mg/ml were applied to glow-discharged 400-mesh Quantifoil grids with 2-μm holes within a carbon support film (Signal Probe Co.). The grids were washed with BrB20, and dialyzed pKinI, incubated with each of ADP, no nucleotide, AMPPNP, and ADP.AlFx, was applied to the grid. The grids were blotted and frozen by plunging them rapidly into liquid ethane slush (Dubochet et al., 1988) and were stored under liquid nitrogen.

Cryo-electron microscopy and helical image analysis

A Gatan coldstage was used for transfer and observation of the frozen grids in a Philips CM200T FEG microscope. Electron micrographs were recorded under low-dose conditions (<10 e/Å^2) at an operating voltage of 120 kV and a nominal magnification of 38,000.

Images of 15-protofilament microtubules for each of pKinI-ADP, -no nucleotide, -AMPPNP, and -ADP.AlFx were chosen visually for image analysis. Selected micrographs were digitized using a flatbed microdensitometer with a step size of 4.97 Å at the specimen. The digitized images were analyzed using standard helical reconstruction methods on Silicon Graphics workstations using the software package PHOELIX (Carragher et al., 1996). An integral number of microtubule repeats were masked off, and Fourier transforms were calculated. Images in each dataset exhibited a range of values of underfocus between 0.95 and 2.2 μm. The contrast transfer function of the microscope was corrected during image processing using PHOELIX. Near- and far-side layer lines with Bessel orders up to ±30 and to an axial resolution of 1/18 Å^{-1} were extracted from the transform of each filament. For each of the pKinI nucleotide three-dimensional maps, datasets were averaged after bringing them to a common phase origin using the strongest layer lines (Bessel orders: 15, −2, 13, −4, 11). Three rounds of phase origin refinement were performed; a microtubule decorated with conventional kinesin motor domain was used as a reference for the first round, while in the second and third cycles, the average from the previous cycle was used. The axial position of the layer lines were refined by two cycles of "sniffing" (Morgan and DeRosier, 1992). Final sets of averaged and sniffed layer lines were truncated to 1/20 Å^{-1}, and three-dimensional maps were calculated using Fourier-Bessel synthesis and summation. We estimate that our maps have a resolution of between 20 and 30 Å. As shown in Fig. S1, the phase information on the equator, and therefore the radial resolution of each map, is good to ∼20 Å. However, the phase information on the 20-Å layer line (−8, 72) is only good in the ADP data, whereas the data on layer line 55 (≡27 Å resolution) is good in all the maps. The following layer lines (*n*, *l*) were used to calculate the final 3D maps where *n* = bessel order and *l* = layer line number: (0, 0); (15, 1); (30, 2); (−17, 17); (−2, 18); (13, 19); (28, 20); (−19, 35); (−4, 36); (11, 37); (26, 38); (−21, 53); (−6, 54); (9, 55); (24, 56); (−23, 71); and (−8, 72). The number of moiré repeats and asymmetric units respectively contributing to each dataset were as follows: ADP 184, ∼26,500; no nucleotide 64, ∼92,00; AMPPNP 58, ∼84,00; and ADP.AlFx 53, ∼76,00.

Difference mapping, contour plotting, and atomic model docking

Difference maps were calculated between each pair of maps, and the statistical significance of any differences was calculated using *t* test (Milligan and Flicker, 1987). To display the contoured projections of individual protofilaments, each map was imported into SPIDER (Frank et al., 1996), and a section through the microtubule wall was cut and contoured. SPIDER was also used to manipulate the pKinI–tubulin AMPPNP projection map. αβ-tubulin dimer atomic coordinates (Löwe et al., 2001; Protein Data Bank identification number 1JFF) and the human conventional kinesin motor core atomic coordinates (Kull et al., 1996; Protein Data Bank identification number 1BG2) were manually docked into the pKinI-ADP microtubule map using AVS (Advanced Visual Systems, Inc.). The contoured maps and the results of the docking experiments were rendered in AVS.

Online supplemental material

The supplemental material (Figs. S1–S3) is available at http://www.jcb.org/cgi/content/full/jcb.200304034/DC1. Fig. S1 shows the steady-state ATPase activity of human Eg5. Fig. S2 shows averaged and sniffed layer lines for each pKinI–microtubule dataset used in the Fourier-Bessel synthesis of the maps shown in Fig. 3. Fig. S3 shows the rate of mantADP release from pKinI.

This work was supported by grants from the National Institutes of Health (GM52468, GM61939, and RR17573).

Submitted: 7 April 2003
Accepted: 30 October 2003

References

Carragher, B., M. Whittaker, and R.A. Milligan. 1996. Helical processing using PHOELIX. *J. Struct. Biol.* 116:107–112.

Crevel, M.-T.C., A. Lockhart, and R.A. Cross. 1996. Weak and strong states of kinesin and ncd. *J. Mol. Biol.* 257:66–76.

Desai, A., and T.J. Mitchison. 1997. Microtubule polymerization dynamics. *Annu. Rev. Cell Dev. Biol.* 13:83–117.

Desai, A., S. Verma, T.J. Mitchison, and C.E. Walczak. 1999. Kin I kinesins are microtubule-destabilizing enzymes. *Cell.* 96:69–78.

Dubochet, J., M. Adrian, J.-J. Chang, J.-C. Homo, J. Lepault, A. McDowall, and P. Schultz. 1988. Cryo-electron microscopy of vitrified specimens. *Q. Rev. Biophys.* 21:129–228.

Frank, J., M. Radermacher, P. Penczek, J. Zhu, Y.H. Li, M. Ladadj, and A. Leith. 1996. SPIDER and WEB: processing and visualization of images in 3D electron microscopy and related fields. *J. Struct. Biol.* 116:190–199.

Goldstein, L.S.B., and A.V. Philp. 1999. The road less traveled: emerging principles of kinesin motor utilization. *Annu. Rev. Cell Dev. Biol.* 15:141–183.

Homma, N., Y. Takei, Y. Tanaka, T. Nakata, S. Terada, M. Kikkawa, Y. Noda, and N. Hirokawa. 2003. Kinesin superfamily protein 2A (KIF2A) functions in suppression of collateral branch extension. *Cell.* 114:229–239.

Huang, T.G., and D.D. Hackney. 1994. *Drosophila* kinesin minimal motor domain expressed in *Escherichia coli*. *J. Biol. Chem.* 269:16493–16501.

Hunter, A.W., and L. Wordeman. 2000. How motor proteins influence microtubule polymerization dynamics. *J. Cell Sci.* 113:4379–4389.

Hunter, A.W., M. Caplow, D.L. Coy, W.O. Hancock, S. Diez, L. Wordeman, and J. Howard. 2003. The kinesin-related protein MCAK is a microtubule depolymerase that forms an ATP-hydrolyzing complex at microtubule ends. *Mol. Cell.* 11:445–457.

Kikkawa, M., E.P. Sablin, Y. Okada, H. Yajima, R.J. Fletterick, and N. Hirokawa. 2001. Switch-based mechanism of kinesin motors. *Nature.* 411:439–445.

Kim, A.J., and S. Endow. 2000. A kinesin family tree. *J. Cell Sci.* 113:3681–3682.

Kline-Smith, S.L., and C.E. Walczak. 2002. The microtubule-destabilizing kinesin XKCM1 regulates microtubule dynamic instability in cells. *Mol. Biol. Cell.* 13:2718–2731.

Kull, F.J., E.P. Sablin, R. Lau, R.J. Fletterick, and R.D. Vale. 1996. Crystal structure of the kinesin motor domain reveals a structural similarity to myosin. *Nature.* 380:550–555.

Löwe, J., H. Li, K.H. Downing, and E. Nogales. 2001. Refined structure of αβ-tubulin at 3.5Å resolution. *J. Mol. Biol.* 313:1045–1057.

Ma, Y., and E.W. Taylor. 1997. Interacting head mechanism of microtubule-kinesin ATPase. *J. Biol. Chem.* 272:724–730.

Maney, T., A.W. Hunter, M. Wagenbach, and L. Wordeman. 1998. Mitotic centromere-associated kinesin is important for anaphase chromosome segregation. *J. Cell Biol.* 142:787–801.

Maney, T., L.M. Ginkel, A.W. Hunter, and L. Wordeman. 2000. The kinetochore of higher eucaryotes: a molecular view. *Int. Rev. Cytol.* 194:67–131.

Maney, T., M. Wagenbach, and L. Wordeman. 2001. Molecular dissection of the microtubule depolymerizing activity of mitotic centromere-associated kinesin. *J. Biol. Chem.* 276:34753–34758.

Milligan, R.A., and P.F. Flicker. 1987. Structural relationships of actin, myosin and tropomyosin revealed by cryo-electron microscopy. *J. Cell Biol.* 105:29–39.

Moores, C.A., M. Yu, J. Guo, C. Beraud, R. Sakowicz, and R.A. Milligan. 2002. A mechanism for microtubule depolymerization by KinI kinesins. *Mol. Cell.* 9:903–909.

Morgan, D.G., and D.J. DeRosier. 1992. Processing images of helical structures: a new twist. *Ultramicroscopy.* 46:263–285.

Niederstrasser, H., H. Salehi-Had, E.C. Gan, C. Walczak, and E. Nogales. 2002. XKCM1 acts on a single protofilament and requires the C terminus of tubulin. *J. Mol. Biol.* 316:817–828.

Nogales, E. 2000. Structural insights into microtubule function. *Annu. Rev. Biochem.* 69:277–302.

Ovechkina, Y., M. Wagenbach, and L. Wordeman. 2002. K-loop insertion restores microtubule depolymerizing activity of a "neckless" MCAK mutant. *J. Cell Biol.* 159:557–562.

Rice, S., A.W. Lin, D. Safer, C.L. Hart, N. Naber, B.O. Carragher, S.M. Cain, E. Pechatnikova, E.M. Wilson-Kubalek, M. Whittaker, et al. 1999. A structural change in the kinesin motor protein that drives motility. *Nature.* 402: 778–784.

Rogers, K.R., S. Weiss, I. Crevel, P.J. Brophy, M. Geeves, and R. Cross. 2001. KIF1D is a fast non-processive kinesin that demonstrates novel K-loop-dependent mechanochemistry. *EMBO J.* 20:5101–5113.

Sack, S., F.J. Kull, and E. Mandelkow. 1999. Motor proteins of the kinesin family: structures, variations and nucleotide binding sites. *Eur. J. Biochem.* 262:1–11.

Sosa, H., D.P. Dias, A. Hoenger, M. Whittaker, E. Wilson-Kubalek, E. Sablin, R.J. Fletterick, R.D. Vale, and R.A. Milligan. 1997. A model for the microtubule-ncd motor protein complex obtained by cryo-electron microscopy and image analysis. *Cell.* 90:217–224.

Turner, J., R. Anderson, J. Guo, C. Beraud, R. Fletterick, and R. Sakowicz. 2001. Crystal structure of the mitotic spindle kinesin Eg5 reveals a novel conformation of the neck-linker. *J. Biol. Chem.* 276:25496–25502.

Vale, R.D., and R.J. Fletterick. 1997. The design plan of kinesin motors. *Annu. Rev. Cell Dev. Biol.* 13:745–777.

Vale, R.D., and R.A. Milligan. 2000. The way things move: looking under the hood of molecular motor proteins. *Science.* 288:88–95.

Walczak, C.E. 2000. Microtubule dynamics and tubulin interacting proteins. *Curr. Opin. Cell Biol.* 12:52–56.

Walczak, C.E., T.J. Mitchison, and A. Desai. 1996. XKCM1: a *Xenopus* kinesin-related protein that regulates microtubule dynamics during mitotic spindle assembly. *Cell.* 84:37–47.

Walczak, C.E., E.C. Gan, A. Desai, T.J. Mitchison, and S.L. Kline-Smith. 2002. The microtubule-destabilizing kinesin XKCM1 is required for chromosome positioning during spindle assembly. *Curr. Biol.* 12:1885–1889.

Wendt, T.G., N. Volkmann, G. Skiniotis, K.N. Goldie, J. Müller, E. Mandelkow, and A. Hoenger. 2002. Microscopic evidence for a minus-end-directed power stroke in the kinesin motor ncd. *EMBO J.* 21:5969–5978.

West, R.R., T. Malmstrohm, C.L. Troxell, and J.R. McIntosh. 2001. Two related kinesins, *klp5+* and *klp6+*, foster microtubule disassembly and are required for meiosis in fission yeast. *Mol. Biol. Cell.* 12:3919–3932.

Wittmann, T., A. Hyman, and A. Desai. 2001. The spindle: a dynamic assembly of microtubules and motors. *Nat. Cell Biol.* 3:E28–E34.

Wordeman, L., M. Wagenbach, and T. Maney. 1999. Mutations in the ATP-binding domain affect the subcellular distributions of mitotic centromere-associated kinesin (MCAK). *Cell Biol. Int.* 23:275–286.